

Diffusion in polymers dependence on crosslink density

Eyring approach to mechanism

Vadim V. Krongauz

NATAS2009 Special Issue
© Akadémiai Kiadó, Budapest, Hungary 2010

Abstract Kinetics of *N*-methyl pyrrolidone evaporation from swollen photo-crosslinked polyacrylate was monitored thermogravimetrically at temperatures ranging from 323 to 398 K. Crosslink density dependence of evaporation kinetics was investigated in photo-crosslinked polyacrylates with crosslinked density ranging from $\approx 1.2 \times 10^2$ to $\approx 1.7 \times 10^4$ mol m⁻³ and number of main chain atoms between crosslinks ranging from ≈ 70 atoms to ≈ 6 atoms, respectively. As was shown, evaporation kinetics was controlled by the solvent diffusion in polymer. Activation energies of evaporation (diffusion) were deduced from the rate measurements at different temperatures. Apparent activation energy of evaporation decreased from 48.7 to 31.1 kJ mol⁻¹ with crosslink density increase. Activation energy of pure *N*-methyl pyrrolidone evaporation was 50.6 kJ mol⁻¹. Decrease of the rate of solvent diffusion and unexpected decrease of diffusion activation energy with increase of crosslink density of swollen polymer matrix was explained by decrease in polymer chain segments mobility, as indicated by Eyring's approach to diffusion in polymers.

Keywords Polymer · Diffusion · Crosslink density · Activation energy · Mechanism · Evaporation · Eyring · Theory · Photo-polymerization

Introduction

Polymers are used in a variety of applications as barriers against liquids and gasses [1], for separation of migrating

molecules according to the rates of diffusion in polymers [2] and as a storage media for diffusion-controlled release of medications, scent, and other active molecules [3]. Kinetics of polymer degradation is believed to be controlled by diffusion of oxygen and volatile degradation products in polymer matrix [4, 5]. Reactions in photopolymers used in electronics and imaging are controlled by the reactants diffusion in polymer matrix [6]. Because of practical and theoretical importance, small molecules diffusion in polymer matrix was extensively studied [7], and several molecular diffusion mechanisms were proposed [7, 8]. Theory of Henry Eyring [8–11] was based on the concepts of free volume and assumption that diffusion proceeds through a transition state involving mutual rearrangement of media molecules and diffusing molecules. It also provided mechanism of diffusion of small molecules in polymers and became the basis for later theories of diffusion of polymeric molecules and diffusion in polymers and polymer monolayers. Eyring theory correlated the rates of molecular diffusion in condensed media with entropy and vibrational and translational energies of molecules. Crosslinking of polymer reduces polymer free volume, solvent absorption and swelling, and the rate of solvent molecules diffusion [7]. All these effects could be explained and quantified using Eyring theory of diffusion, since the structure of transition state of small molecules diffusion in polymer matrix would also change with crosslinking of polymer chains [8–11].

Solvent absorption by polymer and polymer drying are frequently studied diffusion-controlled processes [12–25]. An extent of polymer swelling and shrinking due to absorption and desorption of solvent is controlled by accompanying entropy change (Flory and Huggins, rubber elasticity [26, 27]). A combination of Flory–Huggins Rubber Elasticity Theory and Eyring's Transition State

V. V. Krongauz (✉)
Baxter Healthcare Corporation, Device Center of Excellence,
Applied Science and Technology, Rt. 120 & Wilson Rd.,
RLT-14, Round Lake, IL 60073, USA
e-mail: vadim_krongauz@baxter.com

Theory was elegantly used by Peppas and co-workers to explain molecular mechanism of solvent diffusion in solvent swollen membranes [14–16].

Diffusion rate decrease with crosslink density increase was most often explained by decrease of free volume with crosslinking, creating a perception that diffusion in polymers is somehow analogous to diffusion through narrow channels [7, 12, 15, 22–27]. There are, however, no holes in properly made polymer solids. To understand the diffusion kinetics in polymer matrix, restriction of polymer chains motion should be addressed. Kinetics of diffusion in polymers was also often treated as well understood process in a uniform media [1, 6, 7, 28–33]. However, a number of questions regarding mechanism of molecular motion in and through polymers remained unanswered by experimental and theoretical work [37].

In this work Eyring approach application to swollen polymer networks, pioneered by Peppas and coworkers, was used to explain evaporation kinetics dependence on polymer crosslink density. In particular, the current work was devoted to verification and mechanistic explanation of unexpected, but experimentally observed decrease in activation energy of solvent diffusion in polymer with the increase of polymer crosslink density [24, 25].

From a variety of available methods of diffusion monitoring [7, 28–34], thermogravimetric monitoring of solvent diffusion was selected since it is direct and yields data that allows to a straightforward interpretation [12, 13, 35].

Experimental

Polymer films with different crosslink densities were prepared as described elsewhere [5, 36] by photo-polymerization of resins containing various concentrations of

difunctional (crosslinking) acrylates (Table 1). The completeness of polymerization (>90% acrylates double bond conversion) was verified by acrylates double bond IR absorption at 810 cm^{-1} (Nicolet 8700 FTI Spectrometer Mainframe, Thermo Electron LLC) [36]. The TGA Q 500 (TA Instruments) was used in isothermal mode in all of the experiments on desorption monitoring.

The glass transition temperatures and loss moduli temperature dependence were characterized using dynamic mechanical analysis (DMA) (RSA3, TA Instruments) of 5–6 mm wide, 100–200 μm thick film strips in a tensile mode at 1.0 Hz. Temperature sweep was conducted at $3\text{ }^{\circ}\text{C min}^{-1}$.

The film samples of $\approx 5\text{ mg}$ (prior to swelling) were used in TGA. The films were from 100 to 200 μm thick. To ensure uniform equilibrium distribution of diffusing molecules, the film samples were immersed in *N*-methyl pyrrolidone (NMP) (Burdick & Jackson, spectroscopic grade) for 3 days prior to evaporation kinetics monitoring. High boiling point of NMP, 475 K, ensured that its evaporation (diffusion) could be studied in a broad temperature range. Swollen sample mass varied from ≈ 10 to $\approx 20\text{ mg}$.

The sample thickness was measured before NMP immersion and after 3 days of immersion. The percent swelling was calculated as the difference in thickness of swollen and dry polymer divided by thickness of dry polymer. The TGA measurements were conducted at 323, 348, 373, and 398 K. The TGA oven temperature was increased at 20 K min^{-1} to desired value and maintained until no more sample mass change was observed. The time to drying varied from 30 to 450 min depending on temperature and crosslink density. The experiments were repeated at least twice. Drying of lowest crosslink density polymer was repeated five times at each temperature to ensure, that peculiar drying kinetics presented below was not an artifact. The thermogravimetrically detected

Table 1 Composition of resins forming photocrosslinked acrylate networks

Initiator ^a 651/%	Irgacure 184/%	Oligomer ^a CN966B85/%	Monomer ^a SR256/%	Monomer ^a SR238/%	Total difunctional acrylates (monomer and oligomer) ^b /%
3	2	25	70	0	3.75
3	2	25	60	10	13.75
3	2	25	50	20	23.75
3	2	25	40	30	33.75
3	2	25	30	40	43.75
3	2	25	20	50	53.75
3	2	25	10	60	63.75
3	2	25	0	70	73.75

^a Irgacure 651 (Ciba), α,α -dimethoxy- α -phenylacetophenone; Irgacure 184 (Ciba), 1-hydroxy-cyclohexyl-phenyl-ketone; SR256 (Sartomer), 2(2-ethoxyethoxy)ethyl acrylate; SR238 (Sartomer), 1,6-hexanediol di-acrylate; CN966B85 (Sartomer), urethane acrylate oligomer/monomer blend

^b CN966B85 contains 15% SR238

evaporation kinetic curves coincided with each other within 0–5% (almost identical numerically and coincidental on the graphs).

The initial evaporation rates were deduced from a slope of a linear fit line using PSI Plot software (version 9.01, Poly Software International) as discussed below.

Results and discussion

Polymer swelling upon exposure to compatible solvent and consequent shrinking on drying depends on crosslink density and chain length between crosslinks. The same factors control polymer glass transition and mechanical properties of polymers [26, 27]. Therefore, kinetics of solvent evaporation from swollen polymer networks accompanied by change in chains conformation (polymer volume) should also correlate with crosslink density, as was the case for thermal degradation kinetics [5, 36]. To understand the diffusion mechanism in crosslinked network, the structure of network must be elucidated.

Temperature dependence of elastic response of polymer solids to periodically applied stress yields information on molecular relaxation (Figs. 1, 2) [7, 27, 36, 37]. Consequently, crosslink density influencing molecular relaxation in polymers and glass transition of polymer solids can be deduced from dynamic mechanical analysis results. Glass transition temperatures derived from phase shift, $\tan(\delta)$, between polymer's loss and storage moduli responses to periodic stress at different temperatures, varied from 224.3 to 338.2 K (Fig. 2). The crosslink density of the UV-cured polyurethane acrylates was calculated using experimentally obtained values of the tensile storage moduli at rubbery plateau (Fig. 1) using an expression that followed from Flory's rubber elasticity theory (Fig. 1; Eq. 1; Table 2) [7, 27, 36, 37]:

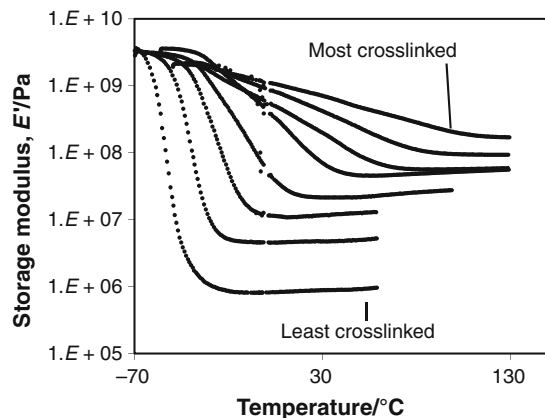


Fig. 1 Dependence of DMA monitored storage modulus of polyacrylate films of different crosslink density on temperature

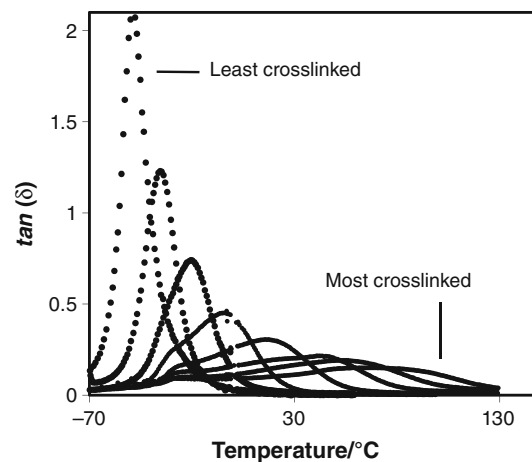


Fig. 2 Determination of glass transition temperatures of crosslinked polyacrylate films from DMA derived $\tan(\delta)$ maxima

$$v_e = \frac{E'}{3RT} \quad (1)$$

where v_e (mol m^{-3}) is a molar concentration of crosslinks, E' (Pa) is tensile storage modulus measured at the rubbery plateau, $R = 8.31 \text{ J K}^{-1} \text{ mol}^{-1}$ is universal gas constant, and T (K) is absolute temperature. Crosslink density derived using Eq. 1 ranged from $\approx 1.2 \times 10^2$ to $\approx 1.7 \times 10^4 \text{ mol m}^{-3}$ (Table 2). The kinetic rubber elasticity theory is not valid for high degrees of crosslinking, and Eq. 1 is valid for polymers with modulus in the range of 2×10^6 to $2 \times 10^8 \text{ Pa}$. Equation 1 yields underestimated crosslink densities for moduli, $E' \gg 2 \times 10^8 \text{ Pa}$. Tensile storage moduli of the polyurethane acrylates studied here were within the range in which the rubber elasticity theory (and Eq. 1) was applicable.

The crosslinked polymer structure may be approximated with the help of Nielsen equation that relates glass transition temperature to concentration of elastic chains [38]:

$$T_g = T_{g0} + \frac{3.9 \times 10^4}{\overline{M}_c} \quad (2)$$

where T_g is crosslinked polymer glass transition temperature, T_{g0} is glass transition temperature of the polymer in non-crosslinked limit, \overline{M}_c is number average molecular weight of the polymer chains between the crosslinks [38–41].

Glass transition in the most crosslinked polymer studied here occurred at $\approx 338.2 \text{ K}$ and in the least crosslinked polymer at $\approx 224.3 \text{ K}$ (Fig. 2; Table 2). Linear extrapolation to 0% concentration of difunctional species yielded $T_{g0} \approx 213 \text{ K}$. Therefore, for most crosslinked polymers studied here $\overline{M}_c \approx 312 \text{ g mol}^{-1}$ and for the least crosslinked, $\overline{M}_c \approx 3450 \text{ g mol}^{-1}$ (Eq. 2). Equation 2 and similar expressions [38–41] are approximations. However, an order of magnitude difference in estimated chain length

Table 2 Physical properties of the UV-cured crosslinked acrylate films

Total difunctional acrylates/%	$T_g/^\circ\text{C}$	Rubberly plateau tensile storage modulus, E'/Pa	Crosslink density $v_e/\text{mol m}^{-3}$	Molecular weight of segment between crosslinks $M_c/\text{g mol}^{-1}$	Backbone atoms number between crosslinks $n_c/\text{atom crosslink}^{-1}$
3.75	-48.7	958809	116	3450	70
13.75	-35.6	5207886	630	1600	30
23.75	-20.6	12956066	1571	1000	20
33.75	-4.8	27467984	2969	710	14
43.75	16.4	55791517	5577	510	10
53.75	43.5	58717987	5875	380	8
63.75	52.9	93323115	9334	340	7
73.75	65.2	170000000	16975	310	6

was deduced for studied polyurethane acrylates indicating a noticeable difference in chain segments mobility in the current range of crosslink densities.

A similar approximation can be used to compute an average number of atoms in polymer backbone between the crosslinks, \bar{n}_c (Eq. 3) [38]:

$$T_g = T_{g0} + \frac{788}{\bar{n}_c} \quad (3)$$

It was found using Eq. 3 that for the least crosslinked polyacrylate $\bar{n}_c \approx 70$ atoms crosslink $^{-1}$ and for the most crosslinked polyacrylate $\bar{n}_c \approx 6$ atoms crosslink $^{-1}$. Molecular weight of the repeating unit between the crosslinks was derived from $\overline{M_c}$ and \bar{n}_c (Eqs. 2, 3), to be $\overline{M_{bc}} \approx 50 \text{ g mol}^{-1}$, a reasonable value for an acrylated moiety (Table 2). The obtained values of molecular weight and chain length of polymer segments between the crosslinks were further used in defining mechanism of molecular diffusion in swollen polymer networks.

The swelling of crosslinked polymers in compatible solvents is a spontaneous process. It is defined by entropy change due to increase in end to end distance of the chains (Eq. 4) [26, 27]:

$$\Delta S(N, R) = \frac{3}{2} \frac{k}{Nb^2} (R_{\text{swollen}}^2 - R_{\text{dry}}^2) \quad (4)$$

where ΔS is entropy change, N number of atoms in main chain segment, k is gas constant, b is Kuhn length ($\approx 14 \text{ \AA}$ for polyethylene), R is an end to end distance in a chain segment. The Eq. 4 illustrates why good solvent absorption is spontaneous, while evaporation requires energy input, and why lightly crosslinked polymers swelling is higher than that of highly crosslinked analog. If one defines swelling as a ratio of thickness after and before solvent absorption, equilibrium swelling (3 days of polymer soaking in NMP) decreased with crosslink density increase and increased linearly with increase in the length of polymer chain between the crosslinks (Table 3; Fig. 3). Thus, expected equilibrium absorption of *N*-methyl pyrrolidone by photo-crosslinked polyurethane acrylates was confirmed.

Although the mass of absorbed solvent is crosslink density dependent decreasing with crosslink density increase (as can be seen from the TGA-detected evaporation, Fig. 4), the dependence of evaporation rate of the absorbed solvent on crosslink density of the polymer is not obvious, and was not studied in detail previously.

Table 3 Polymer swelling (% film thickness change), activation energy of initial evaporation

Crosslink density $v_e/\text{mol m}^{-3}$	Swollen film thickness/dry film thickness	Swelling/%	Apparent activation energy/kJ mol $^{-1}$	Ln(pre-exponent)
0	Solvent	None	50.6	18.8
116	1.56	55.9	48.7	17.8
630	1.27	27.4	42.5	15.8
1571	1.16	16.5	35.9	13.7
2969	1.14	13.5	35.4	13.2
5577	1.22	12.2	34.9	12.8
5875	1.18	18.2	32.0	11.8
9334	1.10	9.9	32.8	11.7
16975	1.06	6.4	31.1	10.9

Fig. 3 Maximum acrylates polymer swelling dependence on **a** crosslink density and **b** on number of backbone atoms between the neighbouring crosslinks

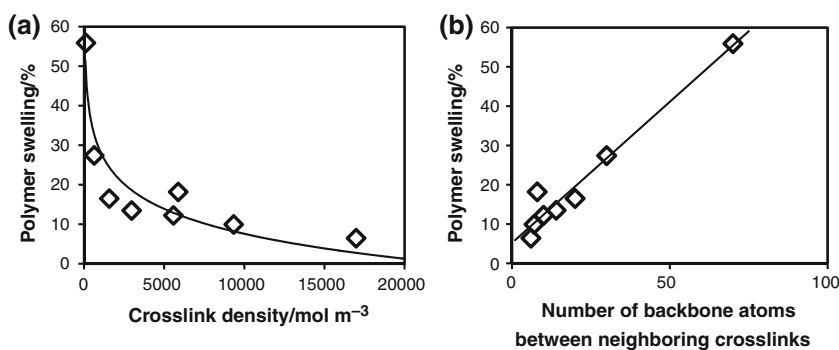
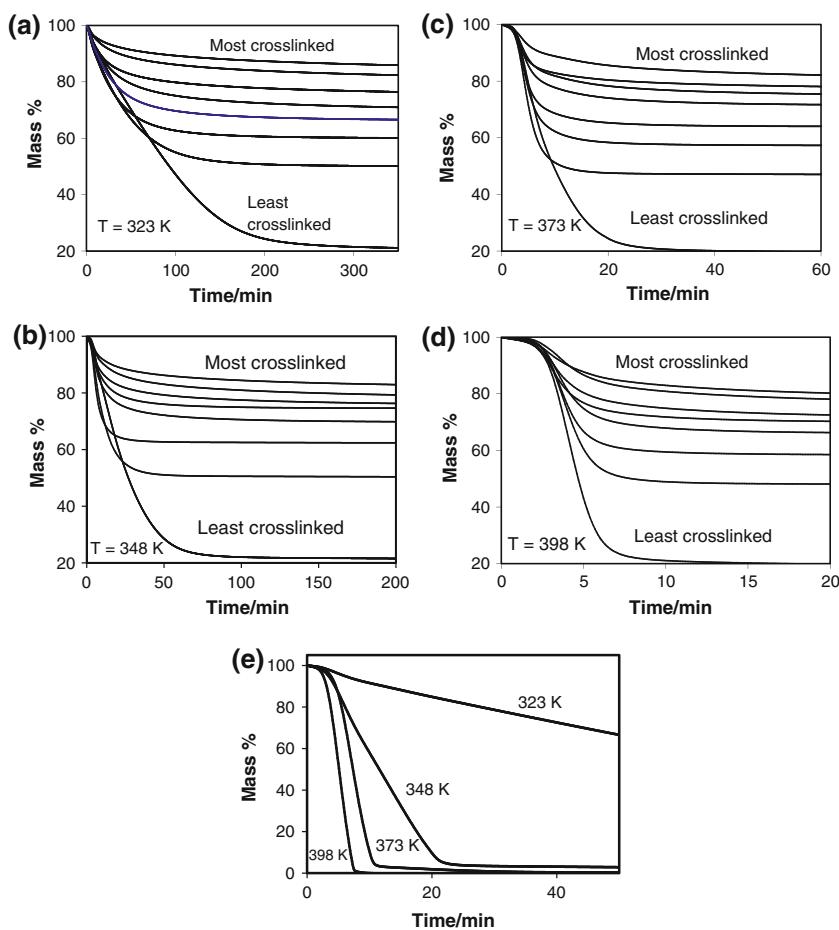


Fig. 4 Weight-detected kinetics of *N*-methylpyrrolidone evaporation. From photo-cured crosslinked acrylate films at temperatures: **a** 323 K, **b** 348 K, **c** 373 K, and **d** 398 K; from a drop of *N*-methylpyrrolidone at: **e** 323, 348, 373, and 398 K



Solvent evaporation from the solvent saturated polymer is accompanied by a change in polymer sample shape, and by time dependent solvent diffusion coefficient [7, 42]. Since absolute values of solvent diffusion coefficients were not sought in the present work, comprehensive numerical modeling of diffusion kinetics to fit an entire length of evaporation kinetics curves, was not conducted [7, 28–33, 42].

The early stages of evaporation could be partially stipulated by evaporation of excess solvent from the polymer

surface. Therefore, the diffusion-controlled evaporation rate was deduced from the linear, middle portions of S-shaped evaporation kinetics curves. To find the “linear” region, inflection point on the middle portion of S shape curve was found and the best linear fit ($y = ax + b$) of 10 points (10 min of evaporation) was conducted using PSI Plot software. The deviation from linearity and difficulty in locating an inflection point on the evaporation kinetics curve resulted in the observed scatter in the rate values. Comparison of the rate computed with five point shift from

the “best” inflection point yielded $\leq 10\%$ error in the deduced slope (rate) values.

The rate of *N*-methyl pyrrolidone (NMP) evaporation derived from the middle, steady portion of S-shaped kinetic curves (Fig. 4) increased with crosslink density increase from $\approx 1.2 \times 10^2$ to $\approx 1.6 \times 10^3 \text{ mol m}^{-3}$ and then decreased with further crosslink density increase at all the studied temperatures (Fig. 5). At 323 K the pure *N*-methyl pyrrolidone evaporation rate (zero crosslink density) was lower than the steady rate of evaporation from swollen polymer with crosslink density $\approx 1.2 \times 10^2 \text{ mol m}^{-3}$ (Fig. 5b). The rate of NMP evaporation from polymers with crosslink density $> 9.3 \times 10^3 \text{ mol m}^{-3}$ was lower than that of the pure NMP at all studied temperatures (Fig. 5b). The differences between the maximum evaporation rate at crosslink density $\approx 1.6 \times 10^3 \text{ mol m}^{-3}$ and that at crosslink density of $\approx 1.7 \times 10^4 \text{ mol m}^{-3}$ at different temperatures far exceeded experimental and computational errors discussed above (Table 4).

Solvent evaporation rate was obtained for polymer films still saturated by solvent, to minimize contributions of the non-equilibrium processes of drying polymer. However, it was possible that observed crosslink dependent differences in evaporation kinetics were influenced by some effect associated with non identical, crosslink dependent change in the polymer surface area. Evaporation rate was normalized to swollen crosslink cell area by division of the rate by square of percentage of thickness increase from dry polymer. Such normalization was justified under traditional assumption that for the films with width and length substantially higher than thickness, area of evaporation changes are due to largest dimensions change. The normalized rate of evaporation at first increased and then declined with crosslink density increase at all studied temperatures (Fig. 6). This qualitative similarity with absolute drying rates indicated that observed evaporation rate dependence on crosslink density was not an artifact induced by

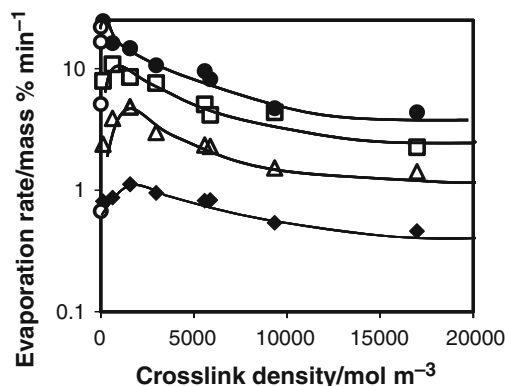


Fig. 5 Crosslink density dependence of the initial rate of *N*-methylpyrrolidone evaporation from swollen polyacrylate films: **a** open circle—initial liquid evaporation rate that corresponds to 0 crosslink density; diamond—initial rate at 50 °C; triangle—initial

Table 4 Comparison of maximum and minimum rates of evaporation

Temperature/ K	Evaporation rate/ mass% min ⁻¹ (crosslink density of $\approx 1.6 \times 10^3 \text{ mol m}^{-3}$)	Evaporation rate/ mass% min ⁻¹ (crosslink density of $\approx 1.7 \times 10^4 \text{ mol m}^{-3}$)
323	1.1	0.5
348	4.8	1.4
373	10.9	2.3
398	24.6	4.4

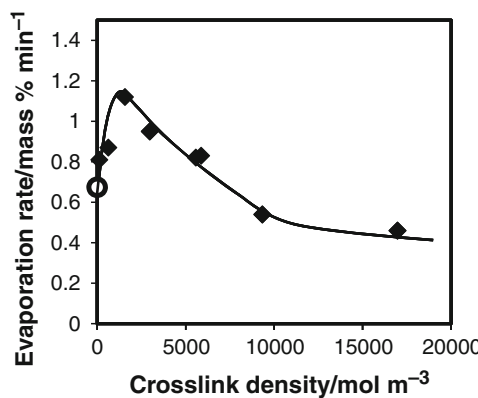
differences in evaporation area change at different crosslinking.

Decrease in evaporation rate with increase in crosslink density from maximum observed to the lowest value was temperature dependent. The ratio of highest and lowest rates of evaporation ranged from a factor of 2.5 at 323 K to 5.6 at 398 K. Since experimental error and error in rate value deduction were in our estimate $< 10\%$, an observed decrease in evaporation rate with degree of crosslinking was well above the experimental error.

Evaporation from polymer consists of diffusion of solvent through polymer to the surface and evaporation from the surface of polymer. Since the rate of weight loss due to *N*-methylpyrrolidone drop evaporation from Pt cup was generally higher (with exception of evaporation at 323 K from lowest crosslink density polymers) than NMP evaporation from swollen polymer, it was concluded that kinetics of evaporation was controlled by the rate of diffusion within the polymer.

Arrhenius-type equation is commonly used to derive diffusion activation energy under the assumption of temperature independence of pre-exponential factor D_0 (Eq. 5; Figs. 7, 8; Table 3):

$$D = D_0 \exp\left(-\frac{\Delta E}{RT}\right) \quad (5)$$



rate at 75 °C; square—initial rate at 100 °C; filled circle—initial rate at 125 °C. **b** Illustration of lowest temperature, 50 °C, evaporation kinetics in linear scale: circle—initial liquid evaporation rate that corresponds to 0 crosslink density; diamond—initial rate at 50 °C

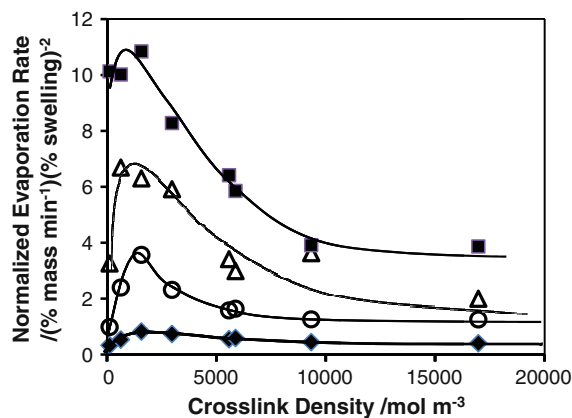


Fig. 6 Crosslink density dependence of evaporation rate normalized with respect to the area of a cell bordered by nearest crosslinks: filled diamond—normalized rate at 50 °C; circle—normalized rate at 75 °C; triangle—normalized rate at 100 °C; filled square—normalized rate at 125 °C

where D is diffusion coefficient, D_0 is pre-exponential factor, ΔE is apparent activation energy of diffusion, R is universal gas constant, T is absolute temperature. The diffusion (evaporation) rate increased with temperature, as expected, for every crosslink density studied (Figs. 3, 5, 6). Apparent activation energy of diffusion in polymer measured in the present work decreased with crosslink density increase (Figs. 9, 10; Table 3), supporting the published results of other researches [24, 25]. To analyze these results mechanism of diffusion in swollen polymer systems was considered.

Eyring explained mechanism of diffusion in condensed media using his transition state theory [7–11] (Eq. 6). Eyring's approach explained that cooperative motion of polymer molecules was required for diffusion in polymers to occur [7, 12–16]. The transition state theory yielded diffusion coefficients described by Eq. 6:

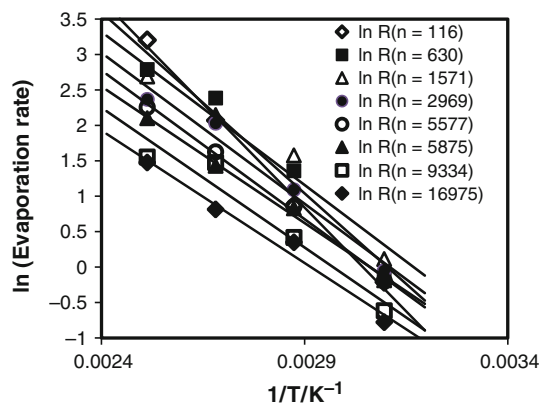


Fig. 7 Initial evaporation rate dependence on inverse absolute temperature for polymers of different crosslink density

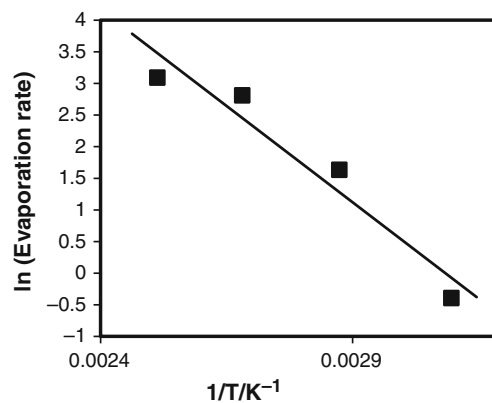


Fig. 8 Dependence of gravimetrically measured rate of *N*-methylpyrrolidone evaporation on inverse absolute temperature

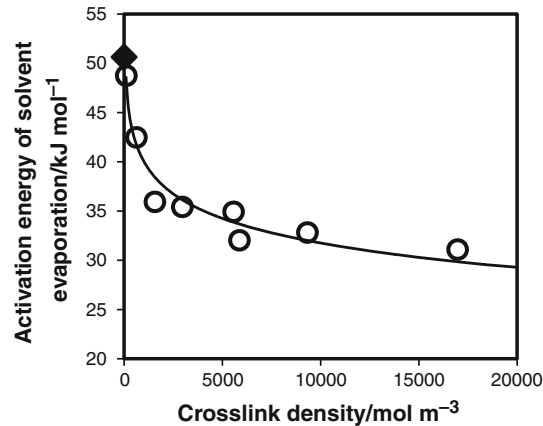


Fig. 9 Dependence of activation energy of evaporation on crosslink density: diamond—pure NMP; circle—in polymer

$$\begin{aligned} D &= \left(\frac{kT}{h}\right)vK^\neq = \left(\frac{kT}{h}\right)v\exp\left(-\frac{\Delta G^\neq}{kT}\right) \\ &= k\left(\frac{kT}{h}\right)\exp\left(\frac{\Delta S^\neq}{R}\right)\exp\left(-\frac{\Delta H^\neq}{RT}\right) \end{aligned} \quad (6)$$

where D is diffusion coefficient, k is Boltzmann constant, h is Plank constant, v is frequency of diffusional jumps, ΔG^\neq is Gibbs energy of combined motion of penetrant and surrounding polymer chains, ΔS^\neq is corresponding entropy change, ΔH^\neq is enthalpy of activation, $k \approx 1$, is “transition coefficient” [7–11]. Diffusion in swollen polymer membranes was also in agreement with Eyring equation (6) [7, 14–16]. Eyring diffusion model requires extension of the chain to accommodate solvent molecules motion. Apparently moving several monomer units to allow diffusion in polymer required more time than motion of small molecules of liquid NMP, since diffusion in swollen polymers was slower than in pure solvent for almost all studied polyacrylates. Apparent activation energy of

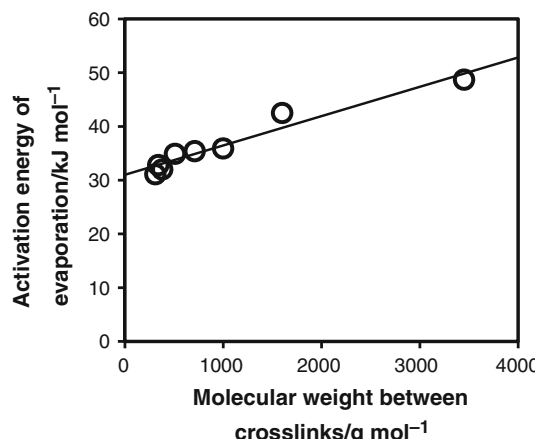


Fig. 10 Evaporation activation energy dependence on molecular weight of chains between the crosslinks

evaporation measured here was higher than apparent activation energies of NMP diffusion in polymers of every studied crosslink density (Table 3; Figs. 8, 9). It can be speculated that energy required for evaporating molecules to overcome surface tension was higher than that required to move weakly crosslinked polymer chains [43–48]. Linear relations between activation energy and molecular weight between crosslinks and activation energy and degree of swelling were found in the current work (Figs. 10, 11).

Combination of Eqs. 6 and 4 can be used to qualitatively explain diffusion coefficient increase with decrease in crosslink density (Eq. 7) [14–16]:

$$\begin{aligned} D &= \left(\frac{kT}{h}\right) v K^\neq \\ &= k \left(\frac{kT}{h}\right) \exp\left(\frac{\frac{3}{2} \frac{k}{Nb^2} (R_{\text{swollen}}^2 - R_{\text{dry}}^2)}{R}\right) \exp\left(-\frac{\Delta H^\neq}{RT}\right) \end{aligned} \quad (7)$$

As indicated by Eq. 7 pre-exponential term determined experimentally decreased with crosslink density increase (Fig. 12). This resulted in decrease of diffusion rate with crosslink density increase.

Experimentally observed decline of activation energy of evaporation from swollen polymer network with increase in network crosslink density, to the best of our knowledge, was not explained previously [24, 25]. To rationalize an observed activation energy decline, let us further separate the terms dependent on polymer volume change from those dependent on molecular interaction (internal energy):

$$\Delta H = \Delta U + p\Delta V \quad (8)$$

where ΔU is internal energy, $p\Delta V$ is the work due to the volume change.

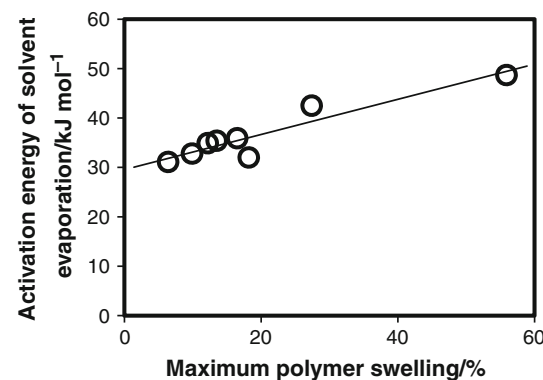


Fig. 11 Dependence of activation energy of *N*-methyl-methyl pyrrolidone evaporation on polymer swelling

The expression can be further expanded using Flory expression for internal energy of mixing of solvent and polymer [26, 27]:

$$\Delta U_{\text{mix}} = \chi\phi(1-\phi)kT \quad (9)$$

where χ is difference in interaction energies in the mixture (Flory interaction parameter), ϕ is repeating polymer unit fraction of total volume of solvent and polymer. Thus,

$$\Delta H_{\text{mix}} = \chi\phi(1-\phi)kT - p\Delta V \quad (10)$$

Then Eqs. 7–10 yield:

$$\begin{aligned} D &= k \left(\frac{kT}{h}\right) \exp\left(\frac{\frac{3}{2} \frac{k}{Nb^2} (R_{\text{swollen}}^2 - R_{\text{dry}}^2)}{R}\right) \\ &\quad \exp\left(-\frac{[\chi\phi(1-\phi)kT + p\Delta V]^\neq}{RT}\right) \end{aligned} \quad (11)$$

Equation 11 does not yield an exact ΔH^\neq dependence on swollen polymer crosslink density, it is safe to assume that the activation volume change due to diffusion, $p\Delta V^\neq$, will be lower in highly crosslinked networks, while monomeric segments interaction, Flory energy, χ will remain the same (the same monomers). The polymer fraction-dependent portion, $\phi(1-\phi)$, passes through the maximum with increase of crosslink density (fraction of polymer units at lower swelling is higher) (Fig. 13). Therefore, at high crosslinking, both, $p\Delta V^\neq$ and $\phi(1-\phi)$ terms will decrease with crosslink density increase, decreasing the activation enthalpy, ΔH^\neq . This indicated that decrease in ΔH^\neq with increase in crosslink density observed in the current and earlier [24, 25] investigations did not contradict and could be explained by the concepts of Flory's polymer swelling thermodynamics and Eyring's diffusion rate theory. Moreover, initial rise and maximum in dependence of diffusion rate in polymer on crosslink density of polymer (Fig. 5) can be explained by a maximum in activation

Fig. 12 Dependence of pre-exponential factor in Eyring's equation of diffusion on polymer crosslink density: *N*-methyl pyrrolidone evaporation from polyurethane acrylates film **a** linear and **b** logarithmic scales

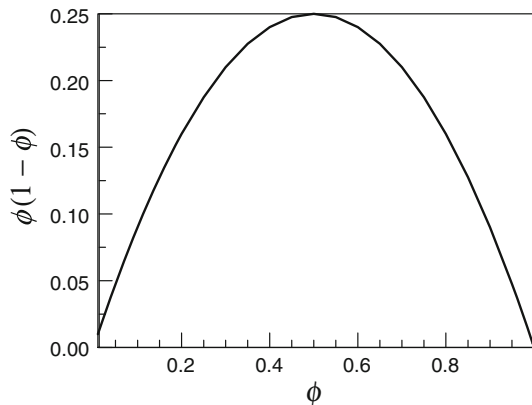
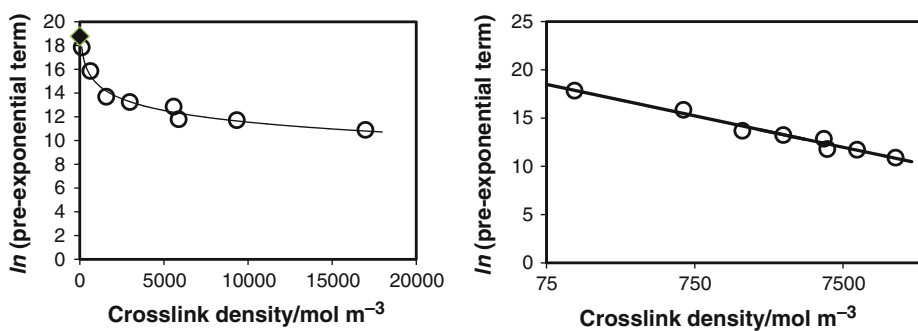


Fig. 13 Polymer fraction-dependent portion of activation enthalpy dependence on polymer fraction in (swollen polymer)–(solvent) system

enthalpy dependence on polymer fraction in swollen polymer–solvent system (Fig. 13). Clearly, further work is required to derive and verify quantitative relations between Eyring diffusion in swollen crosslinked polymeric networks and Flory's statistical theory of rubber elasticity. Remarkable linearity of activation energy dependence on crosslink density and polymer swelling (Figs. 10, 11) and linear dependence of logarithm of pre-exponential factor on logarithm of crosslink density (Fig. 12) also require further consideration and explanation.

Kinetics of small molecules diffusion in polymer monolayers was studied by Langmuir et al., La Mer et al., and Barnes et al. as a function of polymer chain length [43–48]. They applied Eyring's transition state theory and vacancy theory of liquids [7–11] to explain the observed. The approach was named “the energy barrier theory” [45, 48]. It was used to obtain activation energy of water evaporation through aligned dense polymeric monolayers. It was found that activation energy for methylene group, CH₂, movement to form activated complex with water ranges from 0.8 to 1.2 kJ mol⁻¹ [45, 46]. Thus, the activation energy of water diffusion through polymer monolayer increased with the polymer chain length.

In crosslinked polymer matrix one cannot expect to find polymer chains aligned parallel to each other like in

polymer monolayers. However, crosslinked polymer contain not only the chain segments terminated at both ends by crosslink nodes, but also “dangling” polymer chains attached to the network only at one end [27, 49]. Viscoelastic properties of crosslinked polymers, and consequently mobility of chain segments required for solvent diffusion, are strongly dependent on volume fraction of dangling chains. In polymer gel swollen by a compatible solvent, dangling chains are extended into solvent occupied domains. As was shown by Krongauz and co-workers [6, 50–53] and confirmed by Kumar and co-workers [54, 55], in plasticized polymer matrix the dangling chains align along the direction of molecular diffusion. Thus, during solvent absorption and desorption by a film, the orientation of dangling chains perpendicular to the film surfaces may be expected. Thus, we may consider equilibrium diffusion in swollen polymers to some extent similar to diffusion through polymer monolayers. Under this assumption, the solvent diffusion kinetics will depend on confirmation and length of dangling chains [49, 56–58]. The length of crosslink-terminated and dangling chains could be considered equal in first approximation [49], and average length of dangling chains can be found using Eq. 3. Clearly, crosslink density increase in polymers is accompanied by reduction of dangling side chains length [49]. Approximating activation energy of *N*-methylpyrrolidone motion through one CH₂ group of polymer by that of water migration through one CH₂ group of polymer monolayer (from 0.8 to 1.2 kJ mol⁻¹), one obtains for most cross-linked polymer, $n \approx 6$ atoms, $E_a \approx 4.8$ to 7.2 kJ mol⁻¹, while for the least crosslinked polymer, $n \approx 70$ atoms, $E_a \approx 56$ to 84 kJ mol⁻¹. Activation energy of *N*-methylpyrrolidone in acrylates of other levels of crosslinking can be similarly estimated from the data in Table 2. The model of solvent diffusion as that through the diffusion-aligned dangling chains of different length is a gross simplification, yet diffusion activation energy values obtained using water diffusion through monolayers data are of the same order of magnitude as those found experimentally for *N*-vinylpyrrolidone diffusion through swollen polyacrylates. Thus, Langmuir–La Mer–Barnes variation of Eyring theory application would also explain decrease in activation

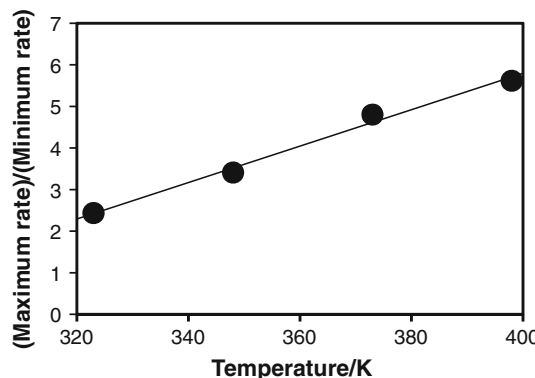


Fig. 14 Temperature dependence of the ratio of maximum solvent diffusion rate at intermediate crosslink density to minimum solvent diffusion rate at maximum crosslink density studied

energy with the crosslink density increase. This approach is more qualitative and debatable than that presented earlier, yet Eyring approach based on co-operative motion of diffusing molecules and molecules of the media again lead to explanation of activation energy decrease with increase of crosslink density, although steeper change of activation energy with crosslink density was obtained.

The ratio of maximum diffusion rate at intermediate crosslink density to minimum diffusion rate at maximum crosslink density studied increased with temperature increase (Fig. 14). This effect was not reported previously and requires further investigation.

In general, further theoretical efforts like those of Amsden [56, 57] and computational modeling similar to recently published ones [58] would be needed for quantitative explanation of the experimentally observed kinetics of diffusion in crosslinked networks. In particular, further work must be directed towards establishing of pre-exponential factors and in defining the degree of dangling chains alignment in thermally drying swollen polymer networks.

Conclusions

Dependence of diffusion kinetics of solvent in solvent swollen crosslinked polyurethane acrylate networks was monitored thermogravimetrically as a function of temperature and crosslink density. Temperature ranged from 323 to 398 K, crosslink density varied from 1.2×10^2 to 1.7×10^4 mol m⁻³. It was observed for the first time that the diffusion rate at first increased and then decreased with crosslink density increase. It was also confirmed that an apparent activation energy of solvent diffusion in swollen polyurethane acrylates matrix decreased with crosslink density increase. The observed behavior was qualitatively consistent with Eyring theory of molecular diffusion [7–11] and Flory rubber elasticity theory [26, 27, 37–41].

It was found that activation energy of diffusion in swollen polymer depends linearly on molecular weight between the crosslinks and on maximum polymer swelling. It was also found that the ratio of maximum diffusion rate at intermediate crosslink density to minimum diffusion rate at maximum crosslink density studied increased with temperature increase.

Acknowledgements Most helpful discussion with Professor Sergey Vayazovkin, University of Alabama at Birmingham, and his valuable suggestion to consider pre-exponential factors behavior added to the diffusion mechanism discussion and are gratefully acknowledged.

References

- Koros WJ, editor. *Barrier polymers and structures*. Washington, DC, USA: ACS; 1990.
- Mulder M. *Basic principles of membrane technology*. The Netherlands: Dordrecht, Kluwer Academic Publication; 1997.
- Rosoff M, editor. *Controlled release of drugs: polymers and aggregate systems*. Weinheim: VCH Verlagsgesellschaft; 1989.
- Wypych G. *Handbook of material weathering*. 3rd ed. Toronto, New York: William Andrew Publication; 2003.
- Krongauz VV, Ling MTK. Photo-crosslinked acrylates degradation kinetics. *J Therm Anal Calorim*. 2009;96:715–25.
- Krongauz VV, Trifunac AD, editors. *Processes in photoreactive polymers*. New York, Tokyo, Toronto, Washington: Chapman & Hall; 1995.
- Crank J, Park GS, editors. *Diffusion in polymers*. New York: Academic Press; 1968.
- Herschfelder JO, Curtis CF, Bird RB. *Molecular theory of gases and liquids*. London, Chichester, Brisbane, Toronto: John Wiley & Sons; 1954.
- Eyring HJ. Viscosity, plasticity and diffusion as examples of absolute reaction rates. *J Chem Phys*. 1936;4:283–91.
- Glasstone S, Laidler KJ, Eyring HJ. *The theory of rate processes*. New York: McGraw Hill; 1941.
- Eyring H, Ree T. Significant liquid structure. VI. The vacancy theory of liquids. *Proc Natl Acad Sci USA*. 1961;47:526–37.
- Errede LA, van Bogart JWC. Polymer drying. II. Replicated time-studies of molecular desorption from liquid swollen poly(styrene-co-divinylbenzene) before and after transition from gel-state to the glass-state. *J Polym Sci A*. 1989;27:2015–49.
- Errede LA. Polymer drying. IV. A molecular interpretation of polymer drying. *J Polym Sci A*. 1990;28:857–70.
- Peppas NA, Reinhart CT. Solute diffusion in swollen membranes. Part I. A new theory. *J Membr Sci*. 1983;15:275–87.
- Reinhart CT, Peppas NA. Solute diffusion in swollen membranes. Part II. Influence of crosslinking on diffusive properties. *J Appl Polym Sci*. 1984;18:227–39.
- Peppas NA, Moynihan HJ. Solute diffusion in swollen membranes. Part IV. Theories for moderately swollen networks. *J Appl Polym Sci*. 1985;30:2589–606.
- Korsmeyer RW, Lustig SR, Peppas NA. Solute and penetrant diffusion in swellable polymers. I. Mathematical modeling. *J Polym Sci*. 1986;24:395–408.
- Korsmeyer RW, Peppas NA. Solute and penetrant diffusion in swellable polymers. II. Verification of theoretical models. *J Polym Sci*. 1986;24:409–34.
- Korsmeyer RW, Peppas NA. Solute and penetrant diffusion in swellable polymers. III. Drug release from glassy poly(HEMA-co-NVP) copolymers. *J Control Release*. 1984;1:89–98.

20. Davidson GWR III, Peppas NA. Solute and penetrant diffusion in swellable polymers. V. Relaxation-controlled transport in P(HEMA-co-MMA) copolymers. *J Control Release*. 1986;3:243–58.
21. Lustig SR, Peppas NA. Solute and penetrant diffusion in swellable polymers. VII. A free volume based model with mechanical relaxation. *J Appl Polym Sci*. 1987;33:533–49.
22. Smith MJ, Peppas NA. Effect of the degree of crosslinking on penetrant transport in polystyrene. *Polymer*. 1985;26:569–74.
23. Robert CCR, Buri PA, Peppas NA. Effect of degree of crosslinking on water transport in polymer microparticles. *J Appl Polym Sci*. 1985;30:301–6.
24. Mateo JL, Bosch P, Serrano J, Calvo M. Sorption and diffusion of organic solvents through photo-crosslinked SBS block copolymers. *Eur Polym J*. 2000;36:1903–10.
25. Zhao C, Li J, Jiang Z, Chen C. Measurement of the infinite dilution diffusion coefficients of small molecule solvents in silicone rubber by inverse gas chromatography. *Eur Polym J*. 2006;42:615–24.
26. Flory PJ. Principles of polymer chemistry. New York: Cornell University Press; 1968.
27. Rubinstein M, Colby RH. Polymer physics. New York: Oxford University Press; 2006.
28. Krongauz VV, Yohannan RM. Photopolymerization kinetics and monomer diffusion in polymer matrix. *Polymer*. 1990;31(6):1130–9.
29. Krongauz VV, Reddy D. Radio-scintillating probe for monitoring molecular transport in polymers. *Polym Commun*. 1990;31(1):7–10.
30. Krongauz VV, Mooney WF III, Schmelzer ER. Interlayer diffusion of small molecules in laminated polymer films. *Polymer*. 1994;35(5):929–34.
31. Krongauz VV, Mooney WF III, Palmer JW, Patricia JJ. New real-time fluorescent probe technique for monitoring diffusion in polymer films. *J Appl Polym Sci*. 1995;56(9):1077–83.
32. Krongauz VV, Chawla CP. Water transport and diffusion in radiation cured coatings and adhesives. RadTech Europe 2001, conference proceedings, October 8–10. 2001; p. 245–252.
33. Ugur S, Yargi O, Pekcan O. Oxygen diffusion into polystyrene-bentonite films. *Appl Clay Sci*. 2009;43:447–52.
34. Hall DB, Miller RD, Torkelson JM. Molecular probe techniques for studying diffusion and relaxation in thin and ultrathin polymer films. *J Polym Sci*. 1997;35:2795–802.
35. Keatch CJ, Dollimore D. An introduction to thermogravimetry. 2nd ed. London, New York, Rheine: Heyden & Son Ltd; 1975.
36. Krongauz VV. Crosslink density dependence of polymer degradation kinetics: photocrosslinked acrylates. *Thermochim Acta*. 2010;503–504:70–84.
37. Sperling LH. Introduction to physical polymer science. 4th ed. London: Wiley; 2006.
38. Nielsen LE. Crosslinking—effect on physical properties of polymers. *J Macromol Sci Rev Macromol Chem*. 1969;3(1):69–103.
39. Katz D, Tobolsky AV. Rubber elasticity in highly cross-linked poly(ethyl acrylate). *J Polym Sci A*. 1964;2(4):1595–605.
40. Tobolsky AV, Takahashi D, Katz M, Schaffhauser R. Rubber elasticity in highly cross-linked systems; crosslinked styrene, methyl methacrylate, ethyl acrylates, and octyl acrylates. *J Polym Sci A*. 1964;2(6):2749–58.
41. Bicerano J, Sammler RL, Craig J, Seitz JT. Correlation between glass transition temperature and chain structure for randomly crosslinked high polymers. *J Polym Sci B*. 1996;34(13):2247–59.
42. Crank J. The mathematics of diffusion. 2nd ed. Clarendon Press: Oxford; 1975.
43. Langmuir J, Schaefer VJ. Rates of evaporation of water through compressed monolayers on water. *J Franklin Inst*. 1943;235:119–62.
44. Archer RJ, La Mer VK. The rate of evaporation of water through fatty acid monolayers. *J Phys Chem*. 1954;59:200–8.
45. La Mer VK, Healy TW, Aylmore LAG. The transport of water through monolayers of long-chain n-paraffinic alcohols. *J Colloid Sci*. 1964;19:673–84.
46. La Mer VK, Healy TW. Evaporation of water: its retardation by monolayers. *Science*. 1965;148:36–42.
47. Quickenden TI, Barnes GT. Evaporation through monolayers—theoretical treatment of the effect of chain length. *J Colloid Interface Sci*. 1978;67(3):415–22.
48. Barnes GT. Permeation through monolayers. *Colloids Surf*. 1997;126:149–58.
49. Curro JG, Pearson DS, Helfand E. Viscoelasticity of randomly cross-linked polymer networks. Relaxation of dangling chains. *Macromolecules*. 1985;18:1157–62.
50. Krongauz VV, Schmelzer ER, Yohannan RM. Kinetics of anisotropic photopolymerization in polymer matrix. *Polymer*. 1991;32(9):1654–62.
51. Krongauz VV, Schmelzer ER. Peculiarities of anisotropic photopolymerization in films. In: Proceeding of SPIE's International Symposium on Optical Application in Science and Engineering, Photopolymer Device Physics, Chemistry, and Application II. 1991;1559:354–376.
52. Krongauz VV, Schmelzer ER. Oxygen effects on anisotropic photopolymerization in polymer matrix. *Polymer*. 1992;33(9):1893–901.
53. Krongauz VV, Legere CC. Morphological changes during anisotropic photopolymerization in films. *Polymer*. 1993;34(17):3614–9.
54. Vorflusev V, Kumar S. Phase-separated composite films for liquid crystal displays. *Science*. 1999;283(5409):1903–5.
55. Wang Q, Park JO, Srinivasarao M, Qiu L, Kumar S. Control of polymer structures in phase-separated liquid crystal-polymer composite systems. *Jpn J Appl Phys*. 2005;44:3115–20.
56. Amsden B. Solute diffusion in hydrogels. An examination of the retardation effect. *Polym Gels Netw*. 1998;6:13–43.
57. Amsden B. Solute diffusion within hydrogel. Mechanism and models. *Macromolecule*. 1998;31:8382–95.
58. Wu Y, Joseph S, Aluru NR. Effect of crosslinking on the diffusion of water, ions and small molecules in hydrogels. *J Phys Chem B*. 2009;113:3512–20.